

Two-Dimensional Wavelet based Medical Videos using Hidden Markov Tree Model

Rubab Fatima Bangash¹

Imran Tauqir

Azka Maqsood

Abstract

Wavelet based statistical image denoising is a vital preprocessing technique in real world imaging. During the acquisition of most medical videos, the device introduces noise, as a result of additional image capturing techniques, resulting in the poor quality of video for examination. So, we required a trade-off between preservation and noise reduction of the actual image content to retains all the necessary information. The existing techniques are based on time-frequency domain where the wavelet coefficients need to be independent or jointly Gaussian. In denoising arena there is a need to exploit the temporal dependencies of wavelet coefficients with non-Gaussian nature. Here we present a YCbCr (Luminance-Chrominance) based denoising strategy on Hidden Markov Model (HMM) that is based on Multiresolution Analysis in the framework of Expectation-Maximization algorithm. Proposed algorithm applies the denoising technique independently on each frame of the video. It models the Non-Gaussian statistics of each wavelet coefficient and captures the statistical dependencies between coefficients. Denoised frames are restored inversely by processing the wavelet coefficients. Significant results are visualized through objectives as well as subjectives analysis. Peak Signal-to-Noise Ratio (PSNR) and Structural Similarity Index Metric (SSIM) parameters are used for the quality assessment of proposed method in comparison with the Red Gray & Blue (RGB) scale video coefficients.

Key Words: Discrete Wavelet Transform, Expectation Maximization, Hidden Markov Tree Model, Video Denoising.

1 Introduction

Video denoising is based on time-frequency data of a video signal. As Far as Image denoising is accomplished by various methods: Time-domain, Frequency-domain, and Time-Frequency combination. Spatial domain methods do not account for the temporal correlation between the frames [1-3]. From an image Spatial noise is being successfully removed by Spatial filters resulting in achievement of high gain failed in restoring the edges particularly in less noisy areas [4]. Time domain techniques considered inter-frame correlation and performed well for motionless videos [5].

Temporal filters failed to remove the noise and produced the fewer blocking artifacts, caused blurring. On the other hand, in case of motioned videos, a temporal filter was not able to give good results in noise removing and delivered fewer blocking artifacts and caused blurring. Hence improved denoising algorithm is need of time, in order to improve the performance of image processing [6-8]

¹National University of Sciences & Technology | fatimabangash@yahoo.com

A new denoising method for medical images e.g. Ultrasound, X-Ray and Magnetic Resonance Imaging (MRI) images, was based on Daubechies Complex Wavelet Transform [9]. Statistical Data Warehouse (SDW) wavelet significantly removed the noise and preserved the details i.e. the local shifts and orientations were preserved with high computational time.

Loizou and Pattichis [10] recommended the DsFlsmv (Mean and variance local statistics despeckle filter), followed by DsFgf4d (Geometric despeckle filtering), and DsFlsminsc (Minimum Seckle Index Homogeneous Mask Despeckle Filter). The proposed method, improved the class separation between the asymptomatic and symptomatic classes. However, due to average filtering, sharp features and noisy boundaries were left unfiltered.

Methods in image denoising is primarily centered around wavelet transform. A denoising technique based on Double Density Dual Tree Complex Wavelet Transform (DDDT-CWT) [11] YCbCr and YUV space was implemented as multi-directional wavelet transform, where the edges and structural contents were restored. However, degradation in performance was seen significantly in real time scenarios.

Medical videos i.e. ultrasound, radiology and capsule endoscopy etc. are subject to noise attenuation. To address this, certain filters are used on ultrasound videos of Common Carotid Artery (CCA) were DsFkuwahara (Despeckling Kuwahara Filter), DsFhmedian (Despeckling Hybrid-Median Filtering), DsFlsmv (Mean and Variance Local Statistics Despeckle Filter) and DsFsrads (Speckle Reducing Anisotropic Diffusion) [12]. Resulting in better visual quality and improved performance in real time videos

Previously, Rabbani Gazor [13] used the Local Bessel K-Form Minimum Mean-Squared Error (BKMMSEL) and Local Bessel K-Form Maximum A-Posteriori (BKMAPL) functions on local Bessel K-Form Density (BKF), for noise free modelling of Three-Dimensional (3D) discrete complex wavelet coefficients in each sub-band. The tested video sequences were corrupted with different types of noises i.e. Additive White Gaussian Noise (AWGN), Poisson, non-stationary and speckle noise. Noise reduction was enhanced with the increased of computational outflow.

Denoising in Computerized Tomography (CT) images was done by another technique, with edge conservation in tetrolet domain (Haar-Type Wavelet Change) [14]. In this a locally adaptive shrinkage rule was applied on high frequency tetrolet coefficients to lessen the noise more viably while preserving the edges and geometrical structures. However, the updated procedure was slow for large objects.

Searching for efficient methods for image denoising is still a challenge. A comparison [15] on the productivity of wavelet based thresholding techniques with presence of speckle noise for different wavelet families i.e. Haar, Morlet, Symlet, Daubechies in de-noising for medical imaging in resonance of brain was proposed. It was found that wavelet transform was proficiently better in analyzing images at various resolutions but the edges were not restored and caused blurring.

A Hidden Markov Tree (HMT) model with 2D-Discrete Wavelet Transform (DWT) was implemented using HMT model in context with Expectation-Maximization algorithm [16] independently on each video frame. Thus, bringing about fast execution with less computational

time, while the improvement needs to be accomplished for enhanced video denoising.

Michele Claus recommended Net (ViDeNN) [17] approach for Video Denoising Thereby, combining two networks, performing first Single Frame Spatial Denoising and subsequently Temporal Denoising over a window of three frames, all in a single feed-forward process. However, the limitations of this method were additional computational power.

Here we have used the above mentioned technique which recommends a spatial-temporal filtering framework that considerably removes speckle noise from images and videos. By exploiting, the dependencies between wavelet coefficients, better performance has been accomplished. The proposed strategy manages the non-Gaussian behavior of wavelet coefficients that are frequently experienced and it gives a proficient outcome for despeckling of images. The results display that the proposed strategy removed noise and it also retained almost all the structural information of each video frame.

In Section-2, the denoised wavelet model is discussed and in section-3, wavelet coefficients are modeled, elaborated by using HMT model. Later in section-4, proposed denoising model is defined. In Section-5 the results of experimentation of proposed model are discussed. In last section, this paper is concluded.

2 Statistical Video Modelling

Wavelet Transform: 2D-DWT has been utilized in numerous restorative imaging applications. Images are decomposed into three level coefficients i.e. several high frequency sub-bands and one low frequency sub-band (LL-sub band) by 2D-DWT (Figure 1). LL-sub band contains the most data in concentrated of highest level known as approximated DWT.

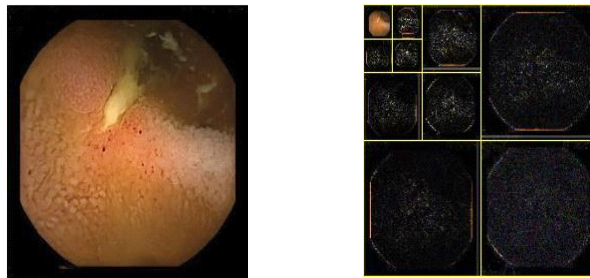


Figure 1: Three Level DWT Decomposition

Hidden Markov Tree Model: When the wavelet coefficients of the images are constructed statistically, HMM captures the Non-Gaussian statistics of these wavelets, matched as Gaussian mixture density (with observed sequence and hidden state). This, consideration of HMM can be labelled as Hidden Markov Tree Model due to the quad-tree nature of wavelets. Wavelet coefficients are linked together with a state variable i.e. every wavelet coefficient was described

by q (a-dimensional state probability) and σ (m-dimensional standard deviation vector).

$$q = (q_1, q_2, \dots, q_m) \quad (1)$$

$$\sigma = (\sigma_1, \sigma_2, \dots, \sigma_m) \quad (2)$$

A multidimensional Gaussian Mixture Model is referred as HMT. Wavelet coefficients are randomly modeled by HMT, with probability density function as a mixture of zero mean Gaussian distribution hidden state for the classification of large and small coefficients. Where pdf of C is:

$$f_c(c) = \sum_{n=1}^N p_Q(n) f_{c|Q}(c|Q=n) \quad (3)$$

Where $p_Q(n)$ is pmf, and Q is a hidden state random variable. Conditional pmf $f_{c|Q}(c|Q=n)$ is given by:

$$f_{c|Q}(c|Q=n) = \frac{2}{\sigma_n \sqrt{2\pi}} \exp\left(-\frac{(b-\mu_n)^2}{2\sigma_n^2}\right) \quad (4)$$

Here μ_n and σ_n are the mean and variance respectively.

HMT used probabilistic tree model to display the Markovian dependencies among hidden states to capture the inter-scale and intra-scale dependencies between wavelet coefficients. For the decomposition of wavelets into u scale and v sub-band, an HMT model has following parameters:

- Standard Deviation = $\sigma_{u,v}$
- Pmf for the root node $Q_i = p_{si}(n)$
- State transition probability matrix of v sub-band from scale $u-1$ to scale $u = A_{u,v}$
- Gaussian mean = $\mu_{u,v}$

The Equation (4) shows state transition matrix as parent \rightarrow children state to state links between the hidden states:

$$A_{u,v} = \begin{bmatrix} p_{u,v}^{y \rightarrow y} & p_{u,v}^{y \rightarrow z} \\ p_{u,v}^{z \rightarrow y} & p_{u,v}^{z \rightarrow z} \end{bmatrix} \quad (5)$$

where or probability of wavelet coefficients to be large or small given its parent is large or small. All these parameters are grouped θ .

$$\theta = [p(\theta_i=n), A_{u,v}, \mu_{u,v}, \sigma_{u,v}] \quad (6)$$

Every wavelet coefficient here, has different state transition probability and variances which

leads toward greater complexity in HMT model. It can be reduced by tying within scale method [19].

3 Denoising Technique

HMT denoising technique with 2D-DWT and 2D-GMM is used. Expectation-Maximization algorithm iteratively find the maximum likelihood from a data set. Our proposed strategy used the adequacy of DWT and the hierarchical relationships between sub-bands. HMT model was used to locate a parameter set θ_q .

A two state GMM was utilized to start the HMT model. At that point, to get θ_q , the inter-scale dependencies were caught by the Markov-tree and EM-algorithm.

Increase in the signal [20] variance is based on added noise while the other parameters are left unchanged. Noisy observation θ_q was extracted and then noise variance was subtracted from it:

$$\left(\sigma_{(u,v,m)n}^{(q)}\right)^2 = \left(\left(\sigma_{(u,v,m)n}^{(q')}\right)^2 - \left(\theta_{(u,v,m)n}^{(q)}\right)^2\right)_+ \quad (7)$$

where v, u and m represent v sub-band, u scale, n state, mth coefficient and

$$\begin{cases} (g)_+ = g & \text{for } g > 0 \\ (g)_+ = 0, & \text{for } g \leq 0 \end{cases}$$

A Model Training via EM Algorithm

EM (Expectation Maximization) algorithm is used for model training. The EM algorithm given in Equation (8), describes the statistical model for hidden state Q and variable C

$$E_{\theta} \left(Q_T(C, Q | C = c) \right) = E_{\theta} \mathcal{D} (c, Q) \quad (8)$$

Conditional pmf of state Q and its maximization is given as:

$$P(Q = n | C, \theta_q) = \frac{P(Q_i) g(C; O, \sigma_{u,v}^2)}{\sum_{i=0}^1 P(Q = l) g(C; O, \sigma_{u,l}^2)} \quad (9)$$

$$P(Q = n) = \frac{1}{N} \sum_{b \in Z^2} P(Q = n | C, \theta_q) \quad (10)$$

After determining θ_q and state probability through HMM, we got $q = E [q | q', \theta_q]$ (Bayes Estimator) can be used to obtain clean coefficients.

$$q = \sum_n (Q|q, \theta_q) \times \frac{\left(\theta_{(u,v,m)_n}^{(q)}\right)^2}{\left(\theta_{(u,v,m)_n}^{(q)}\right)^2 + \left(\theta_{(u,v,m)_n}^{(\epsilon)}\right)^2} q'_{u,v,m} \quad (11)$$

B Inverse Wavelet Transform

Inverse Wavelet Transform (IDWT) is applied in the end to acquire reconstructed video frames. Algorithm for proposed denoising method is summarized in Figure 2.

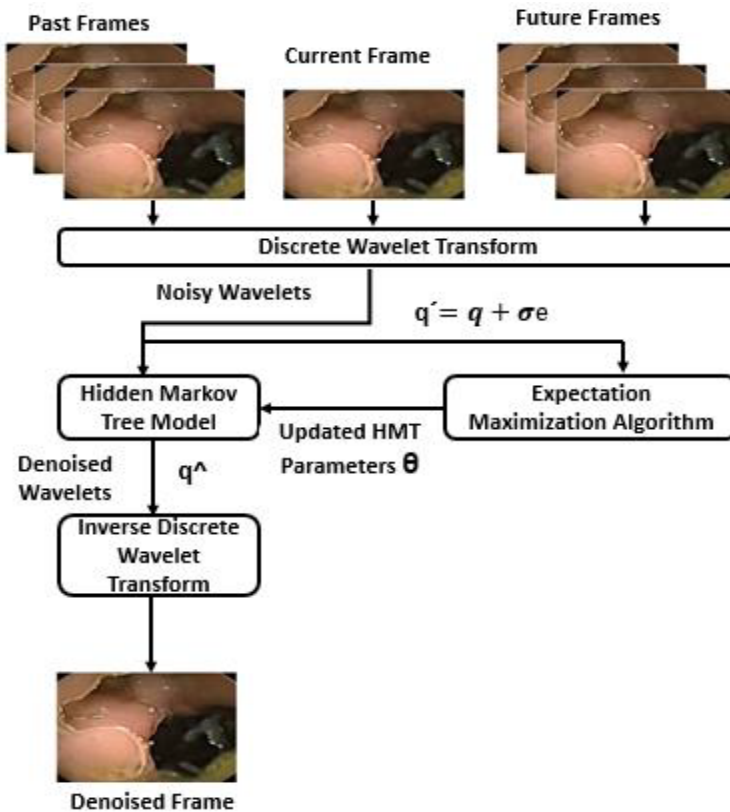


Figure 2: An Overview Proposed Denoising Process

Denoising Algorithm

- Adding noise AWGN in each frame of the video sequence.
- Then applying Daubechies-8 DWT .
- Obtaining DWT coefficients.
- Estimating the GMM parameters.
- Training of HMT model with EM-algorithm in reference to the method of tying within scale.
- Applying IDWT to get reconstructed frames.

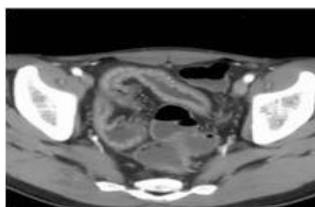
4 Simulations and Results

Each frame of the tested sequence was degraded artificially with speckle noise with noise variances i.e. 0.1, 0.2, 0.3. The sequences were tested in grayscale, RGB and proposed algorithm color space. The analysis of the measurement shown in Table 1 was made on two terms i.e. first on the quantitative performance measure PSNR, secondly on the measurement of perceived image quality with initial noise free image as reference through Structural Similarity Index Measure (SSIM).

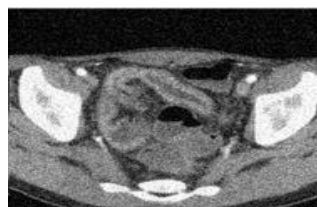
Table 1: Simulation Results

Video Sequences		Grey Scale		RGB		Proposed Algorithm	
		PSNR	SSIM	PSNR	SSIM	PSNR	SSIM
Endoscopy	0.1	21.1167	0.881694	21.1131	0.904999	21.5982	0.884287
	0.2	15.1980	0.822676	15.2762	0.894293	15.5062	0.828196
	0.3	11.6759	0.855640	11.7776	0.909898	11.9761	0.761609
CT Scan	0.1	21.3809	0.866745	21.3847	0.866680	21.5603	0.852319
	0.2	13.9769	0.846671	13.9789	0.867870	15.4741	0.854179
	0.3	11.5437	0.826184	11.4503	0.859014	11.9199	0.837778
Mammogram	0.1	20.0024	0.836505	21.3705	0.867967	21.6039	0.856158
	0.2	13.9792	0.830533	15.1374	0.876485	15.5392	0.846681
	0.3	10.4566	0.831411	11.5517	0.853997	11.9808	0.813299
Ultrasound	0.1	21.1587	0.845638	21.2203	0.905396	21.4992	0.883864
	0.2	13.9793	0.877209	15.3598	0.885453	15.5102	0.864535
	0.3	11.6582	0.848289	11.8212	0.903502	11.9896	0.830726

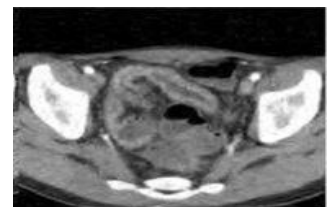
Figures 3(a, d, g) show the noiseless frames of the test sequences, which were later corrupted with speckle noise (Figs. 3(b, e, h)). These frames were then processed through denoising filters to obtain denoised frames (Figs. 3(c, f, i)). Figure 3(j) shows the graphical comparison of the test sequences.



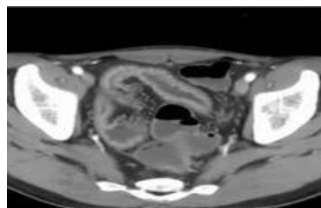
(a) Gray Frame



(b) Noisy Frame



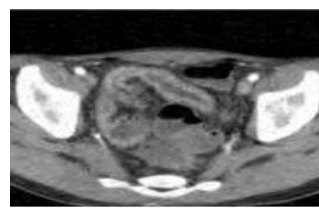
(c) Denoised Frame



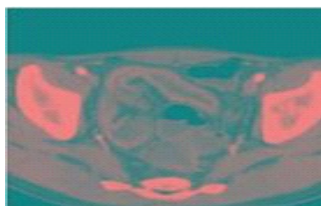
(d) RGB Frame



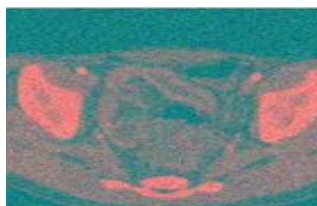
(e) Noisy Frame



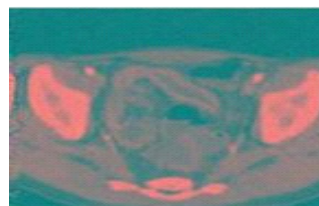
(f) Denoised Frame



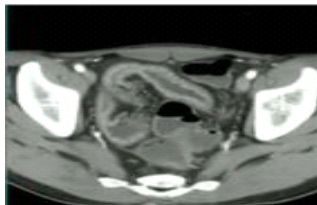
(g) YCbCr Frame



(h) Noisy Frame

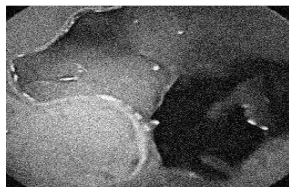


(i) Denoised Frame

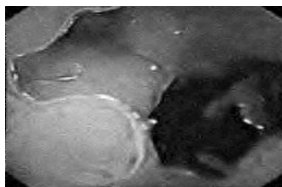


(j) Resulting Recovered Frame

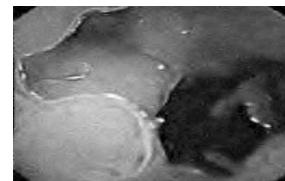
Figures 3: Qualitative Comparison Based on PSNR of CT Scan with Gray Scale (Upper One), RGB Scale (Middle One) and Proposed Algorithm (Last One) View Proposed Denoising Process



(a) Gray Frame



(b) Noisy Frame



(c) Denoised Frame



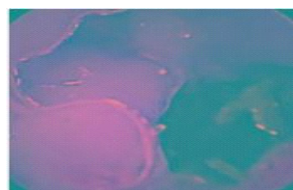
(d) RGB Frame



(e) Noisy Frame



(f) Denoised Frame



(g) YCbCr Frame



(h) Noisy Frame

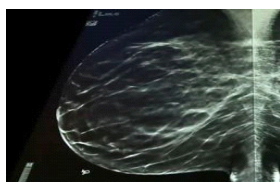


(i) Denoised Frame

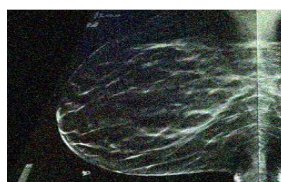


(j) Resulting Recovered Frame

Figures 4: Qualitative Comparison Based on PSNR of Endoscopy with Gray Scale (Upper One), RGB Scale (Middle One) and Proposed Algorithm (Last One) View Proposed Denoising Process



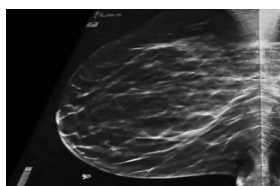
(a) Gray Frame



(b) Noisy Frame



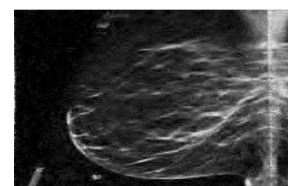
(c) Denoised Frame



(d) RGB Frame



(e) Noisy Frame



(f) Denoised Frame



(j) Resulting Recovered Frame

Figure 5: Qualitative Comparison Based on PSNR of Mammogram with Gray Scale (Upper One), RGB Scale (Middle One) and Proposed Algorithm (Last One) View Proposed Denoising Process

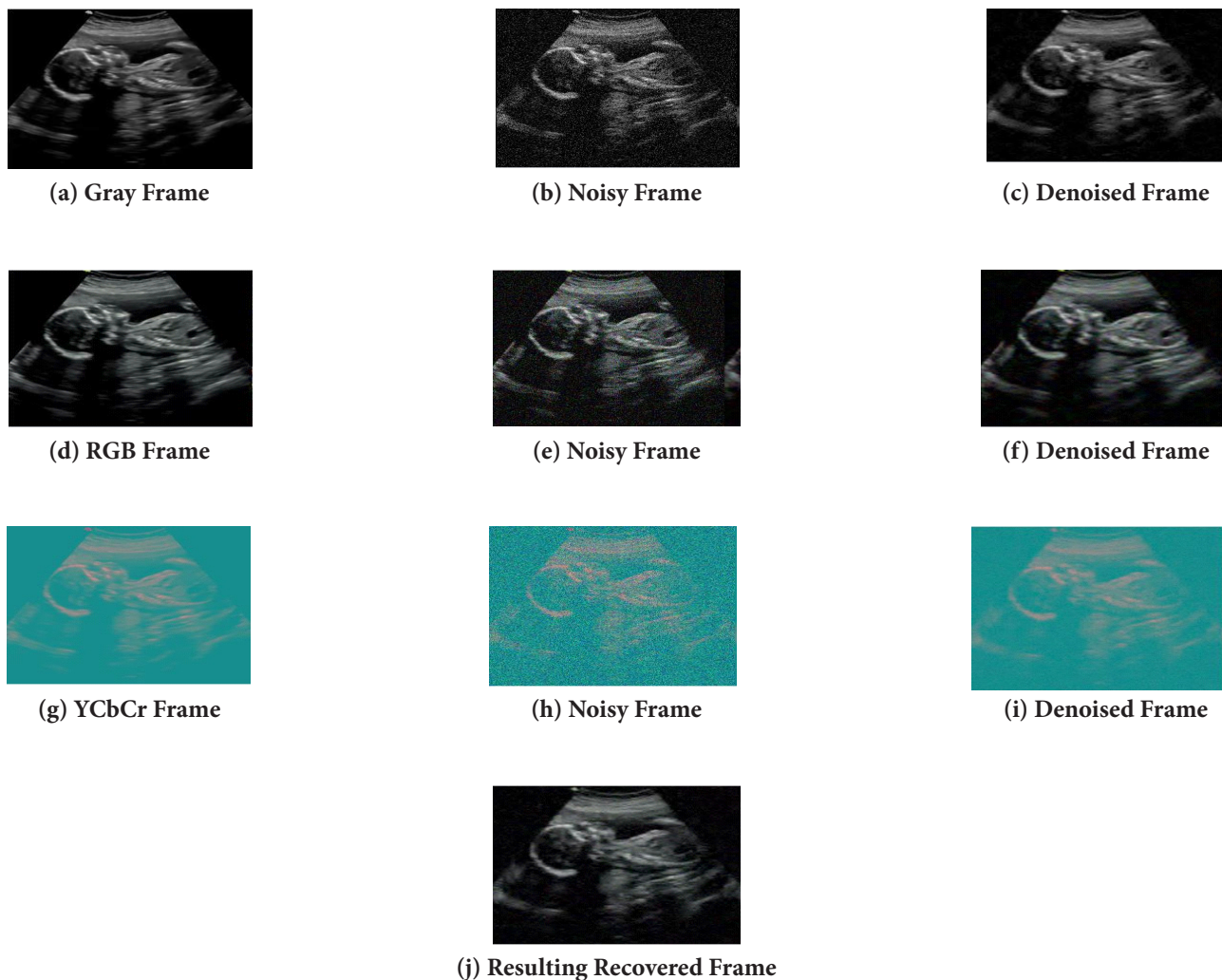
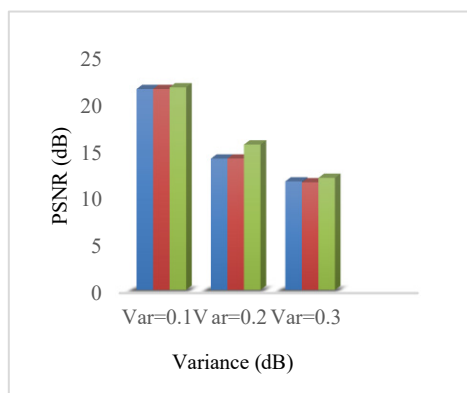
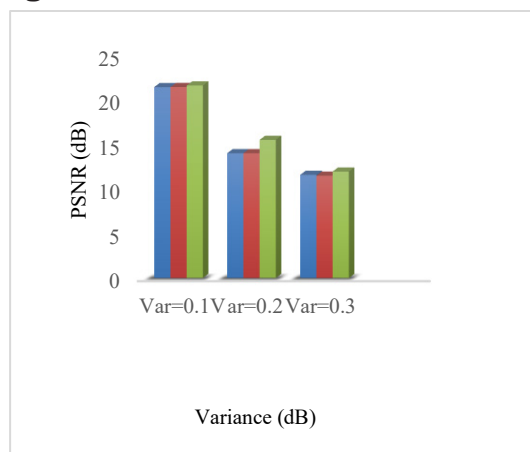


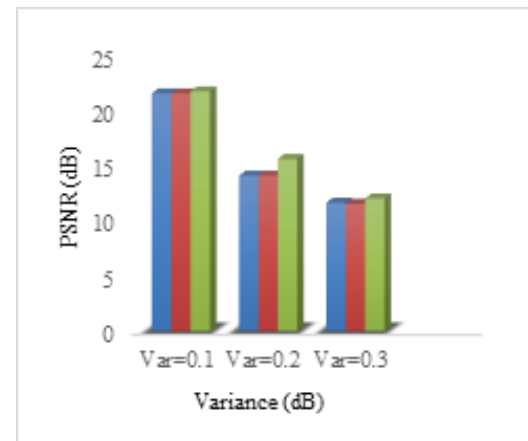
Figure 6: Qualitative Comparison Based on PSNR of ULTRASOUND with Gray Scale (Upper One), RGB Scale (Middle One) and Proposed Algorithm (Last One) View Proposed Denoising Process



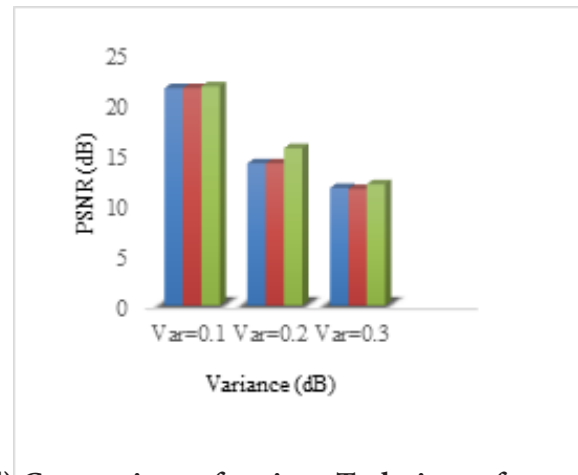
(a) Comparison of various Techniques for CT Scan



(b) Comparison of various Techniques for Endoscopy



(c) Comparison of various Techniques for Mammogram



(d) Comparison of various Techniques for Ultrasound

Figure 7: Graphical Comparison of Different Techniques through PSNR

5 Conclusion

Here we present a wavelet denoising technique based on HMT model with EM algorithm for the despeckling of video frames scale, videos and colored videos in YCbCr color space based on 2D-DWT and 2D-GMM. HMT model was trained by EM algorithm on wavelet coefficients to capture the statistical dependencies present between them. Experimental results revealed that the proposed denoising method performed better in YCbCr space with improved performance up to 0.5dB as compared to gray and RGB space. This method showed improvement in noise reduction, edge preservation and reduced computational complexity. Furthermore, increases in noise variance and using the higher order filter resulted in degraded image quality.

6 Future Work

Proposed denoising scheme can be further extended for the analysis of noises of different variances with other transforms for all color spaces. Moreover, it can be used in other transform domains like Bandelet, Contourlet, Rigdelet and Curvelet in combination with other filters i.e. Bilateral filter. Finally, this technique can be further modified with other techniques for achieving the improved performance and with reduced computational complexity and low latency.

Acknowledgment

This research has been supported by Image Processing Cell, Military College of Signals, National University of Sciences & Technology, Islamabad, Pakistan.

References

- [1] Sharma, A., and Singh, J., December 2013, "Image Denoising Using Spatial Domain Filters: A Quantitative Study", Proceedings of 6th IEEE International Congress on Image and Signal Processing, pp. 293-298, Hangzhou, China.
- [2] Narasimha, C., and Rao, N.A., January 2015, "Spatial Domain Filter for Medical Image Enhancement", Proceedings of IEEE International Conference on Signal Processing and Communication Engineering Systems, pp. 291-295, Guntur, India.
- [3] Wang, B., Xiong, Z., and Zhang, D., October 2014, "Nonlocal Image Denoising via Collaborative Spatial-domain LMMSE Estimation", IEEE International Conference on Image Processing, pp. 2714-2718, Paris, France.
- [4] Lee, J.S., March 1980, "Digital Image Enhancement and Noise Filtering by Use of Local Statistics", IEEE Transactions on Pattern Analysis and Machine Intelligence, Volume 2, pp. 165-168.
- [5] Li, X., Shen, H., and Zhang, L., August 2015, "Sparse-Based Reconstruction of Missing Information in Remote Sensing Images from Spectral/Temporal Complementary Information", International Society for Photogrammetry and Remote Sensing, Volume 106, pp. 1-15.
- [6] Manjón, J.V., Coupé, P., Buades, A., Collins, D.L., and Robles, M., January 2012, "New Methods for MRI Denoising Based on Sparseness and Self-Similarity", Med Image Anal, Volume 16, pp. 18-27.
- [7] Iftikhar, M.A., Jalil, A., Rathore, S., and Hussain, M., March 2014, "Robust Brain MRI Denoising and Segmentation Using Enhanced Non-Local Means Algorithm", International Journal of Imaging System Technology, Volume 24, pp. 52-66, New York, USA.
- [8] Liu, R.W., Shi, L., Huang, W., Xu, J., Yu, C.H., and Wang, D., July 2014, "Generalized Total Variation-Vased MRI RicianDenoising Model with Spatially Adaptive Regularization Parameters", Magnetic Resonance Imaging, Volume 32, pp. 702-720.
- [9] Khare, A., and Tiwary, U.S., October 2007, "Daubechies Complex Wavelet Transform Based Technique for Denoising of Medical images", International Journal of Image and Graphics, Volume 7, pp. 663-687.
- [10] Loizou, C.P., and Pattichis, C.S., January 2008, "Despeckle Filtering Algorithms and Software for Ultrasound Imaging", Morgan & Claypool Publishers, San Rafael, CA, USA Algorithms and Software in Engineering, pp. 1-66.

- [11] Varun, P.G., and Palanisamy, P., January 2012, "Capsule Endoscopic Image Denoising Based on Double Density Dual Tree Complex Wavelet Transform", Article in International Journal of Imaging and Robotics.
- [12] Loizou, C.P, Kasparis, T, Christodoulides, P, Theofanous, C., Pantziaris, M., Kyriakou, E., and Pattichis, C.S., November 2012, "Despeckle Filtering in Ultrasound Video of the Common Carotid Artery", Proceedings of IEEE 12th International Conference on Bioinformatics & Bioengineering, Larnaca, Cyprus, pp. 721-726.
- [13] Rabbani, H., and Gazor, S., December 2012, "Video Denoising in Three-Dimensional Complex Wavelet Domain Using a Doubly Stochastic Modelling", IET Image Processing, Volume 6, pp. 1262-1274.
- [14] Kumar, M., and Diwakar, M., January 2016, "CT Image Denoising Using Locally Adaptive Shrinkage Rule in Tetrolet Domain", Babasaheb Bhimrao Ambedkar University, Lucknow, India.
- [15] Agarwal, S., Singh, O.P, and Nagaria, D., May 2017, "Analysis and Comparison of Wavelet Transforms for Denoising MRI Image", Biomedical & Pharmacology Journal, Volume 10, pp. 831-836.
- [16] Maqsood, A., Tauqir, I., Siddique, A.M., and Haider, M., January 2019, "Wavelet Based Video Denoising using Mehran University Probabilistic Models", Research Journal of Engineering & Technology, 38(1), pp. 17-30, Jamshoro, Pakistan.
- [17] Claus, M., and Gemert, J.V., April, 2019, "ViDeNN: Deep Blind Video Denoising", CVPR Workshops on Computer Science.
- [18] Dass, R., June 2018, "Reduction of Ultrasound Images Using BFO Cascaded with Wiener Filter and Discrete Wavelet Transform in Homomorphic Region", International Conference on Computational Intelligence and Data Science, pp. 1-1866.
- [19] Malfait, M., and Roose, D., April 1997, "Wavelet-Based Image Denoising Using a Markov Random Field a Prior Model", IEEE Transactions on Image Processing, Volume 6, pp. 549-565.
- [20] Crouse, M.S., Nowak, R.D., and Baraniuk, R.G., April 1998, "Wavelet-Based Statistical Signal Processing using Hidden Markov Models", IEEE Transactions on Signal Processing, Volume 46, pp. 886-902.
- [21] Golshan, H.M., Hasanzadeh, R.P., and Yousefzadeh, S.C., September 2013, "An MRI Denoising Method Using Image Data Redundancy and Local SNR Estimation", Magnetic Resonance Imaging, Volume 31, pp. 1206-1217.